Z. Phys. D – Atoms, Molecules and Clusters 12, 319–326 (1989)

Atoms, Molecules
Zeitschrift für Physik D and Clusters

Electronic structure of metal clusters

G.K. Wertheim
AT&T Bell Laboratories, Murray Hill, NJ 07974, USA

Received 5 July 1988; final version 30 September 1988

Photoemission spectra of valence electrons in metal clusters, together with threshold ionization potential measurements, provide a coherent picture of the development of the electronic structure from the isolated atom to the large metallic cluster. An insulator-metal transition occurs at an intermediate cluster size, which serves to define the boundary between small and large clusters. Although the outer electrons may be delocalized over the entire cluster, a small cluster remains insulating until the density of states near the Fermi level exceeds 1/kT. In large clusters, with increasing cluster size, the band structure approaches that of the bulk metal. However, the bands remain significantly narrowed even in a 1000-atom cluster, giving an indication of the importance of long-range order.

The core-electron binding-energy shifts of supported metal clusters depend on changes in the band structure in the initial state, as well as on various final-state effects, including changes in core hole screening and the coulomb energy of the final-state charge. For cluster supported on amorphous carbon, this macroscopic coulomb shift is often dominant, as evidenced by the parallel shifts of the core-electron binding energy and the Fermi edge. Auger data confirm that final-state effects dominate in cluster of Sn and some other metals. Surface atom core-level shifts provide a valuable guide to the contributions of initial-state changes in band structure to cluster core-electron binding energy shifts, especially for Au and Pt. The available data indicate that the shift observed in supported, metallic clusters arise largely from the charge left on the cluster by photoemission. As the metal-insulator transition is approached from above, metallic screening is suppressed and the shift is determined by the local environment.

PACS: 79.60; 36.40

Introduction

The fundamental goal of cluster studies is to elucidate the size-dependent atomic and electronic structure of clusters ranging in size from the isolated atom to the bulk metal. The structural and electronic properties are, of course, intimately coupled. The electronic structure depends on the spatial arrangement of the atoms, and the equilibrium spatial structure depends on the ability of the resulting electronic bands to accommodate the outer electrons. First principles calculations to determine the equilibrium structure of few-atom clusters have been carried out for small Na [1] and Si [2] clusters, among others.

Many of the interesting phenomena that occur in clusters arise from the transition from bonds to bands with increasing cluster size. For elements that are metals in the bulk there will be a transition from insulator to metal with increasing cluster size. Since this phenomenon occurs in all the systems discussed here, it is important to have a clear understanding of what constitutes metallic behavior. Phenomenologically a metal is defined by its ability to conduct an electric current and by the positive temperature coefficient of its resistivity. These properties depend on the presence of a conduction band intersected by the Fermi level, which make it possible to excite electron-hole pairs of all energies, no matter how small. This is

the fundamental criterion which defines a metal. All the properties which are unique to metals depend on such a partially filled band. The presence of electronic states delocalized over all the atoms of a cluster is a necessary, but not a sufficient condition to make it a metal.

The transition from insulator to metal takes place when the density of electronic states in the vicinity of the Fermi level is high enough so that the levels overlap by virtue of the thermal width [3]. The critical cluster size for the transition to the metallic state, estimated on this basis, falls in the vicinity of 100 atoms for an alkali metal at room temperature. For compact Al clusters the development of the conduction band has been calculated for clusters of 13, 55, and 147 atoms [4], showing a rapid convergence toward a bulk-like conduction band.

Cluster growth

Most of the data to be discussed here were obtained with clusters grown on a substrate, typically sputter-cleaned amorphous carbon. The metal atoms are usually deposited from a Knudsen cell onto a room temperature substrate, and have sufficient mobility to nucleate $\sim 3 \times 10^{12}$ clusters/cm^2 during the early stages of the deposition [5, 6]. The number of atoms in the average cluster is obtained by dividing the coverage by the density of nucleation sites. The average volume and radius can then be readily obtained. Continued deposition results in growth of these clusters, leading ultimately to coalescence into a contiguous metallic layer, but one which typically has holes. Since the cohesion of the cluster atoms is much greater than their adhesion to the substrate, the clusters will be compact and will tend to have a faceted, spherical shape. The mass of each cluster is proportional to the amount of material deposited per unit area of the substrate, up to the point where coalescence becomes significant. The cluster diameter consequently varies as the cube root of the coverage, Θ. Small regions of this relationship have been approximated by a linear behavior, but the average cluster diameter is never proportional to the coverage. Confirmation of the growth and coalescence of clusters was recently obtained from the coverage-dependence of the core electron binding energy and signal intensity [7].

Electron spectroscopy of clusters

We begin by considering the contribution of electron spectroscopy to our understanding of the electronic structure of clusters.

1. Threshold ionization potential

The smallest photon energy capable of ejecting an electron from a cluster locates the highest occupied molecular orbital (HOMO) relative to the vacuum level. Measurements on small alkali metals clusters show a rapid initial drop of this threshold ionization potential (IP) from the single atom to the few-atom clusters, followed by a continued slow decrease in many-atom clusters [8–10]. These results are in good accord with a shell-model calculations in which the nuclear and inner electronic charge is treated as jellium [11, 12]. The outer electrons are delocalized over the entire cluster, but have discrete energy levels and exhibit shell-closure effects (magic numbers) analogous to those of the nuclear shell model. These are in good accord with experimental observations. The model also reproduces the even-odd fluctuations found in alkali atom clusters. For the range of cluster sizes typically studied in beam experiments, the clusters are not metallic by the criterion established above. The combination of measurement and theory for the few-atom cluster leads to a simple picture for the behavior of the outer electrons, which are destined to become the conduction electrons in the larger, metallic cluster.

In large metallic clusters the threshold ionization potential approaches the work function of the bulk metal from above with increasing cluster size. The difference between the threshold IP of a free cluster and the work function of the bulk metal is equal to the coulomb energy $e^2/2r$ of the charged cluster. (The cluster has unit positive charge in the final state due to the emission of the electron.) An image-charge model had earlier led to the conclusion that this term has the form $3e^2/8r$ [13, 14], but an analysis based on energies is more reliable. For small metallic clusters, with band structures significantly different from that of the bulk metal, there will also be changes in the chemical potential and in the surface dipole layer [15].

In general then, as we form clusters starting with the isolated atom, progressing through the molecular and metallic cluster to the bulk metal, the threshold ionization potential decreases from the first ionization potential of the free atom of the work function of the bulk metal. The states of the outer electrons are delocalized but remain discrete until the density of states becomes so high that they overlap by virtue of their thermal width, forming a band. If this band is not fully occupied metallic behavior obtains. The threshold IP follows a $1/r$ law in the metallic region. The size below which this law breaks down may be identified with the metal-insulator transition. These simple measurements combined with suitable theory provide a great deal of insight into the behavior of the out-

ermost electrons of clusters of metal atoms. For more detailed information about the electronic structure we must turn to a more sophisticated spectroscopy.

2. *Photoemission spectroscopy of valence bands*

In order to observe the electronic structure in greater detail one determines the kinetic energy distribution of the electrons excited by photons with energy well above the IP threshold. In spite of the multitude of phenomena that modify the details of this spectrum, it corresponds in first order to the distribution of occupied electronic states, both core and valence.

The most immediate application is the measurement of valence band density of states. Such data have consistently shown a narrowing of the bulk metal bonds, when the metal is in the form of small clusters [16–21], Fig. 1. The measured band widths are typically monotonically related to the cluster size, and to parameters like the average coordination number, which provide a quantitative measure of the difference between a cluster and the bulk metal. In model calculations for simple metals the bandwidth is proportional to the square root of the coordination number [22]. The band narrowing at the surface of metals is in rough agreement with this prediction, so that one might expect it to be applicable to large metallic clusters, which one can visualize as a core of bulk-like metal surrounded by a surface-like layer. However, one should not extrapolate this "law" from the large metallic cluster all the way to the molecular clusters with small average coordination numbers.

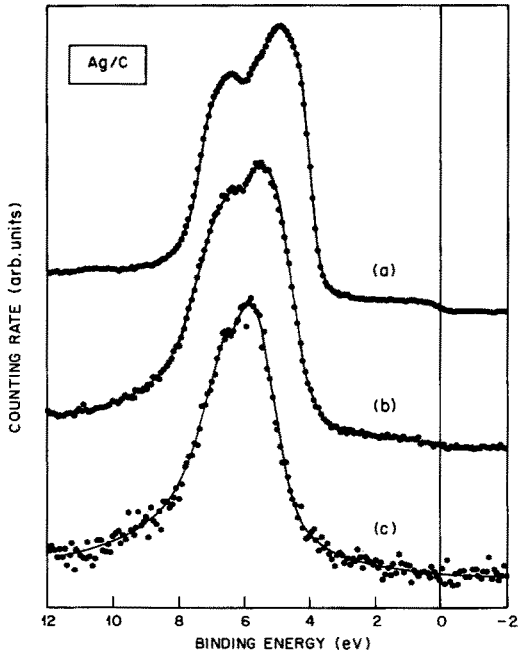

Fig. 1. X-ray photoelectron spectra of the valence bands of bulk silver, and Ag clusters at coverages of 1.0×10^{15} and 2.5×10^{14} atoms/sm^2 on amorphous carbon. The substrate signal has been subtracted. (from Ref. 27)

X-ray photoelectron spectroscopy of the valence bands of random-sized supported clusters shows not only an over-all narrowing, but also a loss of the detailed features characteristic of the bulk solid. Since this effect is seen in quite large clusters, it is not readily explained by the presence of different cluster sizes, but must be due to the loss of long-range periodicity. Recent measurements with relatively small, size-selected supported Au clusters [23] show the 5*d* band approaching a broadened spin-orbit doublet. It is not yet clear whether this broadening should be attributed to 5*d*-5*d* overlap or to the inequivalent atomic sites in the cluster. Significant progress in valence band spectroscopy has also been made in pulsed laser-excited photoemission from small, free Cu clusters, in which individual 4*s* electron states were resolved [24].

Under favorable conditions, photoemission can provide more detailed information about the structure of the valence bands. For example, for a planar polycrystalline surface, the band structure of the surface atoms can be separated from that of the bulk simply by changing the take-off angle [25]. It is unfortunately impossible to apply this techniques to supported clusters. All we can obtain is a total density of valence band states for all the atoms in the cluster. Nevertheless, the information obtained from surface layers on bulk crystals is relevant to the interpretation of cluster properties. For a 100 atom cluster, with a diameter typically near 10Å, 80 percent of the atoms are part of the surface. An appreciable fraction of these are edge atoms, which should have properties even further removed from those of the bulk than the surface atoms. To a low order of approximation one might then expect to be able to predict the changes observed in the valence band of large clusters in terms of those found in the bulk and at the surface of macroscopic solids, using the fraction of bulk and surface atoms in the cluster as a guide.

3. *Photoemission from core levels*

Core-electron spectra are more easily obtained by XPS than valence band spectra, because the lines are narrower and the core electrons have larger cross sections. A great deal of work focusing on the core-electron binding-energy shift has been reported for clusters of simple, noble, transition, and rare earth metals. The remarkable fact is that in every case the core-electron binding energy is larger in the cluster than in the metal,

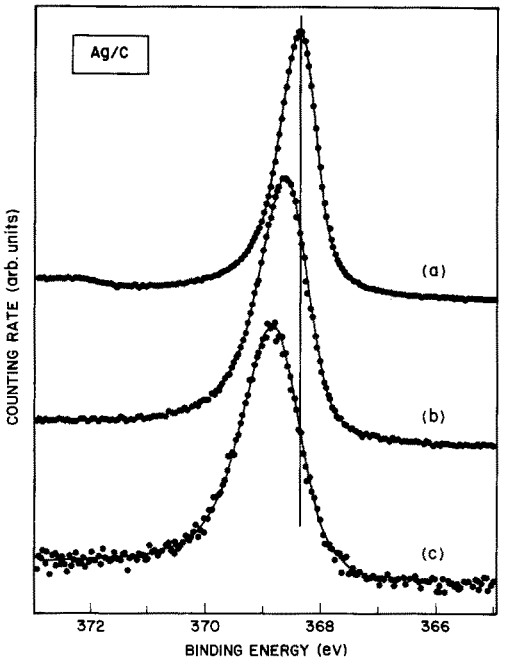

Fig. 2. The Ag $3d_{5/2}$ core electron spectra of samples shown in Fig. 1. (from Ref. 27)

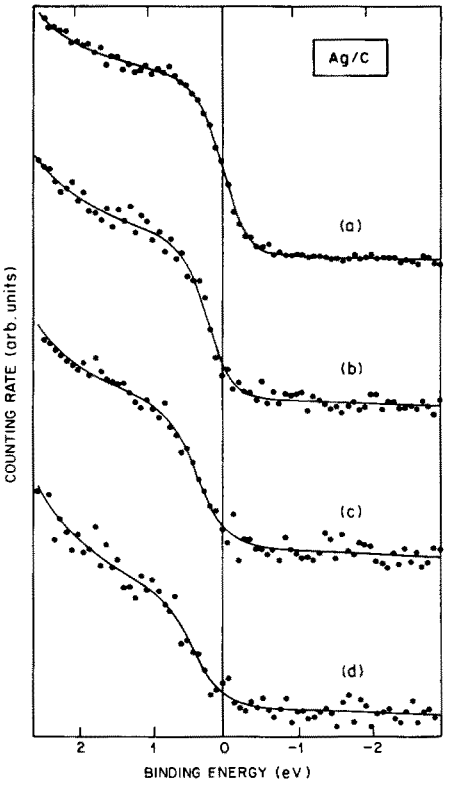

Fig. 3. Shift of the Fermi edge of small supported Ag clusters relative to that of the amorphous carbon substrate. (from Ref. 27)

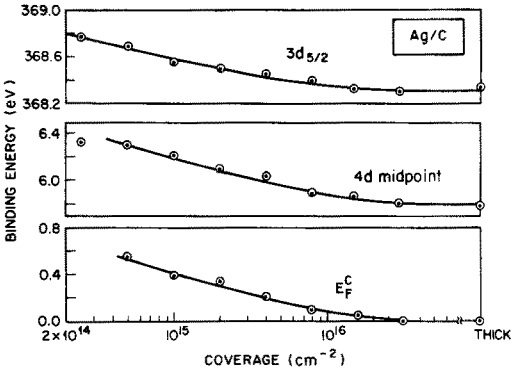

Fig. 4. Comparison of Fermi edge, valence band, and core level shifts of supported Ag clusters. (from Ref. 27)

increasing monotonically with decreasing cluster size, as illustrated in Fig. 2. This is traceable simply to the fact that photoemission may leave even a supported cluster with unit positive charge in the final state [26]. However, depending on cluster size, other mechanisms will also contribute. Included here are (1) a reduction of the screening in the final state, and (2) changes in band structure resulting in a redistribution of charge between orbitally-distinct bands in the initial state. For supported clusters the substrate interaction will also have to be considered.

For large, *isolated* metal clusters the analysis is simple. The core hole is screened by the conduction electrons much as it is in the bulk metal. The resulting charge-deficit in the conduction band appears at the surface of the cluster, making the final result quite similar to that encountered in the discussion of the threshold IP. The energy of the final state is increased by $e^2/2r$ relative to that of the infinite metal, correspondingly reducing the kinetic energy of the photoelectron, and increasing the core-electron binding energy. Confirmation that this mechanism is dominantly responsible for the core-level shift comes from the comparison of the shifts for the core electron and the cluster Fermi level [26, 27], see Figs. 3 and 4. It should be noted that for the smaller clusters the shift of the 3*d* electrons is smaller than the Fermi edge shift. This is due to changes in band structure that add a small negative components, i.e., a shift with the same sign as the surface atom core-level shift of silver. This is in accord with the increase of the surface to volume ratio with decreasing cluster size. The band structure contribution to the shift should in general have the same sign as the surface-atom core-level shift, e.g. positive for transition metals with less than half-filled *d*-shell, and negative for those with more than half-filled shell.

For *supported* metal clusters the energy of the final state of the system is reduced to about 1/2 by the

formation of an image of the charged cluster in the substrate. For grounded clusters, e.g. clusters supported on a metallic substrate, this shift will vanish [26, 28].

In small, metallic clusters conduction electron screening will be suppressed if the coulomb energy of the charged cluster ($e^2/2r$) exceeds the energy reduction afforded by the core-hole screening process [28–30]. Consequently, the macroscopic coulomb shift will never exceed the relaxation energy in the bulk metal. Metals with a small density of states at E_F, and hence small small screening energies, will have small cluster core-electron binding-energy shifts.

In smaller, non-metallic clusters conduction electron screening is replaced by the polarization of the neighboring atoms or even by the transfer of a valence electron to the atom with the core hole. The final state is more localized, and no longer depends strongly on cluster size. In these clusters the screening will be a function of the neighbor environment (coordination number), so that one may expect inhomogeneous broadening of the core-electron photoemission line. In this regime the core-electron binding-energy shift is not equal to the change in threshold IP.

Theoretical calculations of core-electron binding energy shifts have so far been reported only for small, nonmetallic cubical Li clusters [31]. They show the expected decrease in binding energy with increasing cluster size, and demonstrate that atoms with different local environment have distinct core-electron binding energies. The calculated range of energies is, however, much larger than one would find in real clusters, because the model includes corner atoms with very low coordination number [32]. These shifts are described as having an initial state origin, while those measured in our experiments are clearly due to final state effects. The authors of [31] see this as a fundamental contradiction. However, experiment and theory are concerned with different regimes of cluster size, metallic vs. molecular, so that they are not directly comparable.

4. Auger electron spectroscopy

The kinetic energy of Auger transitions between core levels depends on the initial state band structure and the final state relaxation. The same contributions appear in the core-electron binding energy obtained by photoemission. In the Auger process the relaxation term has a coefficient of 3, because the initial state has one core hole and is singly charged, while the final state has two and is doubly charged. This makes it possible to combine core-electron binding energy shifts with Auger kinetic energy shifts to separate the initial and final state contributions [33]. Core-valence-valence Auger transitions cannot be used in this analysis, because the final state screening of a valence hole is inherently different from that of a core hole. In this analysis, the effect of charge left on a cluster by photoemission is not distinguishable from that of final state relaxation [34]. Limited attempts to use this formalism to identify the initial and final state contributions to core-electron binding energy shift indicate that final state effects dominate [20, 34].

Case studies

We will now examine some of the available data for a number of different metals to illustrate and expand on the points raised above. We begin with a particularly simple case.

1. Tin

In Sn the conduction band consist of 5*s* and 5*p* states, with limited opportunity for charge flow between bands with greatly different radial distribution. The magnitude of the surface atom core level shift is much less that 0.1 eV. The 3*d* core electron binding energy Sn clusters supported on amorphous carbon follows the 1/r behavior expected on the basis of the final state charge [7, 29, 35], see Fig. 5. No information about the electronic structure is consequently obtained from

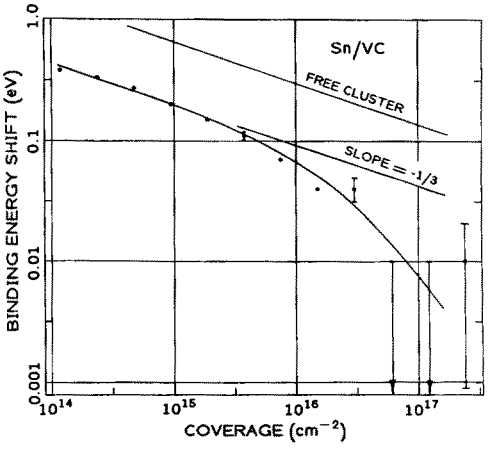

Fig. 5. Core-electron binding energy shift of tin clusters on vitreous carbon plotted against coverage. For coverages less than 3×10^{15} cm^{-2} the data exhibit a slope of $-1/3$, indicating that the shift is inversely proportional to the linear dimension of the clusters. At higher coverage the shift drops rapidly below this line indicating that the clusters have begun to coalesce. The coulomb shift for free clusters of the same diameter is also indicated. (from Ref. 7)

core level studies, but the results confirm that the final state charge is the source of the observed core level shifts. Auger data support the final-state nature of the shift [34].

2. *Silver*

In Ag the 4*d* band lies in the interval from 4 to 7.5 eV below the Fermi level. The density of states at E_F is much smaller than in Sn. The surface atom core level shift is small, i.e., −0.08 eV [25]. As we have already seen in Fig. 1, the Ag 4*d* valence band narrows significantly and remains well below E_F as the cluster size is decreased. The 4*d* band, consequently, remains filled, so that there is no flow of charge between the 4*d* and 5*s* bands. The largest observed 3*d* cluster core-level shift is smaller than that in Sn, reflecting the smaller density of states. The observations are fully accounted for by the cluster charge [7, 27].

3. *Gold*

In Au the 5*d* band lies in the interval between 2 and 7.5 eV below E_F. The surface-atom core-level shift is −0.4 eV, i.e. toward smaller binding energy [25]. The 5*d* band is narrowed at the surface, and exhibits a centroid shift comparable to the core-level shift. In the clusters the *d*-band is also narrowed, but the shifts are toward larger binding energy with decreasing cluster size. The data do not conform to the behavior of Sn or Ag when plotted as in Figs. 4. A reasonable interpretation is that initial-state effects produces a shift toward smaller binding energy, i.e., with the same sign as the surface atom shift, which competes with the effect of the cluster charge, resulting in a more complicated size-dependent shift. No attempt has so far been made to separate these two contributions.

Recent experiments with size-selected Au clusters [23] have given band widths comparable to those of random-sized clusters with the same average diameter, indicating that the width is an inherent property of the individual cluster, and not due to the size distribution. This is reasonable if the width is due to residual *d-d* interactions. The structure of the valence band spectra is no more detailed than that of random-sized clusters. Core electron spectra, Fig. 6, also exhibit shifts and broadenings comparable to those of random-sized clusters. The broadening of the core levels is, however, much smaller than that of the valence band, and probably reflects the inequivalence of the atoms within each cluster. The interaction with the substrate undoubtedly makes an important contribution to this inequivalence of the various atoms in the cluster.

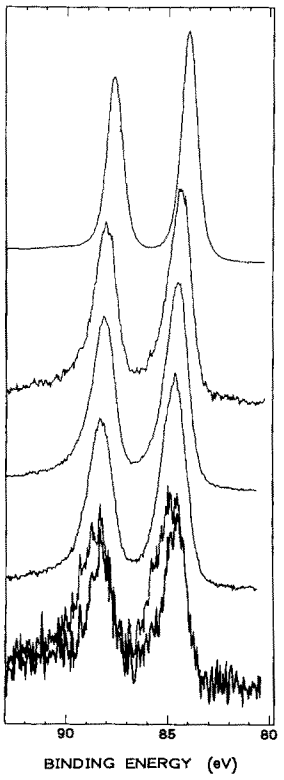

Fig. 6. XPS spectra of the Au 4f electrons of size-selected, supported Au clusters. The upper curve is for bulk gold, those below for clusters of 33, 27, 7, and "5" atoms. (from Ref. 23)

4. *Palladium*

In Pd the 4*d* band is intersected by the Fermi level. There would consequently appear to be ample opportunity for charge redistribution between it and the 5*s* conduction band. However, charge flow between the bands can only come about by the motion of the two band relative to each other [27]. Narrowing of the almost filled 4*d* band will move the top edge away from the vacuum level. Narrowing of the almost empty 5*s* band will move its charge toward the vacuum level. The net result of the narrowing of both bands will be a transfer of charge into the 4*d* band moving the system toward the $4d^{10}$ configuration of the free Pd atom. The position of the Fermi level after band-narrowing will be largely determined by the motion of the top of the high-density-of-states 4*d* band. On the basis of these considerations one would expect a negative surface-atom core-level shift, but this has not been experimentally established. Our own attempts to measure the shift were unsuccessful, and indicated only that it is much smaller than that of Au.

The narrowing of the 4*d* valence band in Pd clusters has been known for many years [16, 17]. The valence-band data also show that the *d* band moves

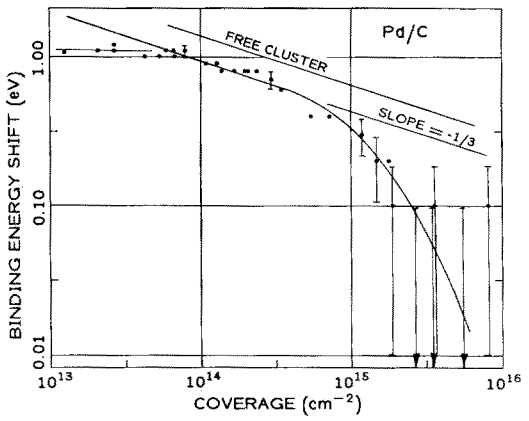

Fig. 7. Core-electron binding energy shift for Pd clusters, from Ref. 37, replotted as in Fig. 3. Note the saturation of the shift below a coverage of 10^{14} cm^{-2}, where the average clusters contains fewer than 30 atoms. (from Ref.7)

away from the Fermi level of the substrate with decreasing cluster size. If it were not for the effect of the final state charge, the separation of the *d*-band from E_F would be a clear indication of a transition to an insulating state. (A filled 4*d* band implies an empty 5*s* band.) The core-level shift toward larger binding energy with decreasing cluster size is also well established [20, 27, 36, 37]. The sign of the shift is opposite to that expected from the increased *d*-band occupancy, and is again best explained in terms of the final-state charge. The 3*d* binding energy shift, Fig. 7, conforms quite well to the predictions of the cluster charge model, lending considerable weight to that interpretation, and confirming that the band structure contribution to the shift is small. The data are unique in clearly showing a leveling off in the limit of small clusters, presumably corresponding to the transition to the non-metallic state in which the 5*s* band is empty.

Auger data have been interpreted as supporting an initial state origin for the Pd cluster shift [37]. However, since this work is based on a final state with two valence band holes, the conclusion is invalid [34].

5. *Platinum*

Platinum, the 5*d* analog of Pd, exhibits similar behavior. XPS data show that the valence band narrows and loses some of its barely resolved structure in small clusters. The loss of the sharp peak at E_F has been interpreted as indicating a loss of occupied 5*d* density [20], but is more likely due simply to the change in the band structure of a finite cluster. The size dependence of the core-electron binding energy shift conforms quite well to the predictions of the final-state cluster charge model [7], although a significant contribution from changes in band structure should be present.

Conclusions

Threshold ionization potentials provide only limited information about the development of the electronic structure of clusters. For small, insulating clusters the threshold IP can be interpreted in terms of the shell-model. For large, metallic clusters it reflects the coulomb energy of the charged final state. Valence band photoemission spectra have clearly demonstrated the narrowing of the bands in metallic clusters. More detailed information about valence bands is only now beginning to emerge from the study of size-selected clusters, both free and supported. Core-level binding energy shifts are dominated by the effects of the charged final state, and shed little light on the electronic structure. Currently major interest is focused on the metal-insulator transition, which is expected for clusters in the 7 to 10Å range, and appears to have been observed for supported Pd clusters.

I am indebted to S.B. DiCenzo for permission to use the unpublished results in Fig. 6, as well as for a critical reading of this manuscript.

References

1. Martins, J.L., Buttet J., Car, R.: Phys. Rev. Lett. **53**, 655 (1984)
2. Raghavachari, K., Logovinsky, V.: Phys. Rev. Lett. **55**, 2853 (1985); see also Blaisten-Barojas, E., Levesque, D.: Phys. Rev. B. **34**, 3910 (1986)
3. Kubo, R., Kawabata, A., Kobayashi, S.: Ann. Rev. Mater. Sci. **14**, 49 (1984)
4. Casula, F., Andreoni, W., Maschke, K.: J. Phys. C. **19**, 5155 (1986)
5. Hamilton, J.F., Logel, P.C.: Thin Solid Films **16**, 49 (1973); **23**, 89 (1974)
6. DiCenzo, S.B., Wertheim, G.K.: Comments Solid State Phys. **11**, 203 (1985)
7. Wertheim, G.K., DiCenzo, S.B.: Phys. Rev. B **37**, 844 (1988)
8. Rohlfing, E.A., Cox, D.M., Kaldor, A.: Chem. Phys. Lett. **99**, 161 (1983)
9. Powers, D., Hansen, S.G., Geusic, M.E., Michalopolous, D.L., Smalley, R.E.: J. Chem. Phys. **78**, 2866 (1983)
10. Knight, W.D., Clemenger, K., deHeer, W.A., Saunders, W.A., Chou, M.Y., Cohen, M.L.: Phys. Rev. Lett. **52**, 2141 (1984)
11. Ekardt, W.: Phys. Rev. B. **29**, 1558 (1984)
12. Beck, D.E.: Solid State Commun. **49**, 381 (1984)
13. Smith, J.M.: AIAA J. **3**, 648 (1965)
14. Wood, D.M.: Phys. Rev. Lett. **46**, 749 (1981)
15. Plieth, W.J.: Surf. Sci. **156**, 530 (1985)
16. Unwin, R., Bradshaw, A.M.: Chem. Phys. Lett. **58**, 58 (1978); Takasu, Y., Unwin, R., Tesche, B., Bradshaw, A.M., Grunze, A.M.: Surf. Sci. **77**, 219 (1978)
17. Egelhoff, W.F., Tibbetts, G.G.: Solid State Commun. **29**, 53 (1979); Phys. Rev. B **19**, 5028 (1979)
18. Oberli, L., Monot, R., Mathieu, H.J., Landolt, D., Buttet, J.: Surf. Sci. **106**, 301 (1981)

19. Lee, S.T., Apai, G., Mason, M.G., Benbow, R., Hurych, Z.: Phys. Rev. B **23**, 505 (1981)
20. Mason, M.G.: Phys. Rev. B **27**, 748 (1983), and references therein
21. Colbert, J., Zangwill, A., Strongin, M., Krummacher, S.: Phys. Rev. B **27**, 1378 (1983)
22. Cyrot-Lackmann, F.: Adv. Phys. **16**, 393 (1967); J. Phys. Chem. Solids **29**, 235 (1968)
23. DiCenzo, S.B., Berry, S., Hartford, E.: Phys. Rev. B **38**, 8465 (1988)
24. Smalley, R.E.: Bull. Am. Phys. Soc. **33**, 642 (1988)
25. Citrin, P.H., Wertheim, G.K., Baer, Y.: Phys. Rev. Lett. **41**, 1425 (1978); Phys. Rev. B **27**, 3160 (1983)
26. Wertheim, G.K., DiCenzo, S.B., Youngquist, S.E.: Phys. Rev. Lett. **51**, 3210 (1983)
27. Wertheim, G.K., DiCenzo, S.B., Buchanan, D.N.E.: Phys. Rev. B **33**, 5384 (1986)
28. Wertheim, G.K., DiCenzo, S.B., Buchanan, D.N.E., Bennett, P.A.: Solid State Commun. **53**, 377 (1985)
29. Cini, M.: Surf. Sci. **62**, 148 (1977)
30. Castellani, N.J., Leroy, D.B., Lambrecht, W.: Chem. Phys. **95**, 459 (1985)
31. Parmigiani, F., Kay, E., Bagus, P.S., Nelin, C.J.: J. Electron Spectrosc. Relat. Phenom. **36**, 257 (1985)
32. DiCenzo, S.B., Wertheim, G.K.: J. Electron Spectrosc. Relat. Phenom. **43**, c7 (1987)
33. Wagner, C.D.: Faraday Discuss. Chem. Soc. **60**, 291 (1975)
34. Wertheim, G.K.: Phys. Rev. B **36**, 9559 (1987)
35. Cheung, T.T.P.: Chem. Phys. Lett. **110**, 219 (1984)
36. Cheung, T.T.P.: Surf. Sci. **127**, L129 (1983); ibid. **140**, 151 (1984)
37. Kohiki, S., Ikeda, S.: Phys. Rev. B. **34**. 3786 (1986)